LIMNOLOGY AND OCEANOGRAPHY
Letters

ASLO
Open Access

Limnology and Oceanography Letters 8, 2023, 509–518

doi: 10.1002/lol2.10314

LETTER

Potential drivers and consequences of regional phosphate depletion in the western subtropical North Pacific

*Zhongwei Yuan,[1,2] Thomas J. Browning,[2] Ruifeng Zhang,[3] Chengwang Wang,[1] Chuanjun Du,[4] Yanmin Wang,[1] Ying Chen,[5] Zhiyu Liu,[1] Xin Liu,[1] Dalin Shi,[1] Minhan Dai[1]**

[1]State Key Laboratory of Marine Environmental Science & College of Ocean and Earth Sciences, Xiamen University, Xiamen, China; [2]Marine Biogeochemistry Division, GEOMAR Helmholtz Centre for Ocean Research, Kiel, Germany; [3]School of Oceanography, Shanghai Jiao Tong University, Shanghai, China; [4]State Key Laboratory of Marine Resource Utilization in South China Sea, Hainan University, Haikou, China; [5]Shanghai Key Laboratory of Atmospheric Particle Pollution Prevention, Fudan University, Shanghai, China

Scientific Significance Statement

Concentrations of phosphate, an essential nutrient for phytoplankton growth, are depleted across a large extent of the western subtropical North Pacific. However, the drivers and consequences of this are still not well constrained. We investigated this with field and satellite observations, shipboard experiments, and model estimates of aerosol nutrient supply across a major phosphate gradient in this region. Collectively these data suggested that phosphate depletion was primarily driven by enhanced nitrogen fixation rates stimulated by aerosol iron, in turn supplying biologically available nitrogen without a corresponding supply of phosphate. The impact of observed phosphate depletion was enhanced microbial utilization of the more abundant dissolved organic phosphorus pool.

Abstract

In regions of the nitrogen limited low latitude ocean, phosphate can also be depleted to levels initiating stress responses in marine microbes. Here, we associate a broad region of phosphate depletion in the subtropical North Pacific with different levels of phosphorus stress. Nutrient and aerosol addition experiments demonstrated primary nitrogen limitation of the bulk phytoplankton community, with supply of aerosols relieving this limitation. At northern sites with depleted phosphate, alkaline phosphatase activities were enhanced, indicating elevated phosphorus stress. Analysis of satellite- and model-derived aerosol loading showed that aerosol deposition was elevated in these regions. Surface rate measurements suggested that the regional enhancement in phosphate depletion was predominantly driven by elevated

*Correspondence: mdai@xmu.edu.cn

Associate editor: Jeffrey W. Krause

Author Contribution Statement: MD, ZY, and TJB designed the research. ZY and RZ performed the experiments. ZY conducted the alkaline phosphatase activity analyses. ZY and YW conducted the macronutrient analyses. CD and ZL calculated nutrient diapycnal fluxes. CW conducted the trace metal analyses. RZ and XL conducted the chlorophyll *a* measurements. DS oversaw the N_2 fixation rate measurements. YC conducted the aerosol measurements. ZY, TJB, and MD drafted the manuscript. All authors discussed and commented on the manuscript.

Data Availability Statement: Biogeochemical data collected onboard used in this study are available on the Science Data Bank (https://www.scidb.cn/s/RryEVf).

Additional Supporting Information may be found in the online version of this article.

nitrogen fixation, likely stimulated by the coincident supply of aerosol iron. Such observations are important for predicting future biogeochemical responses in the subtropical North Pacific to changing aerosol supply.

Nitrogen (N) limits phytoplankton growth throughout the majority of the low latitude oceans, but in certain regions phosphate (DIP) can be depleted to levels approaching colimitation (Moore et al. 2013). Most evidence for DIP depletion has been provided from the (sub)tropical North Atlantic, where numerous studies have demonstrated that DIP concentrations can be depleted to < 10 nmol L^{-1}, levels leading to microbial phosphorus stress (Wu et al. 2000; Mather et al. 2008; Moore et al. 2008, 2009; Van Mooy et al. 2009; Mahaffey et al. 2014; Browning et al. 2017). However, evidence has also accumulated for low DIP concentrations over a broad extent of the (sub)tropical North Pacific (Hashihama et al. 2009, 2021; Kitajima et al. 2009; Shiozaki et al. 2010; Martiny et al. 2019; Browning et al. 2022). This has important implications for projecting future changes of the broad oligotrophic North Pacific ecosystems, given the fact that DIP concentrations have been suggested to be declining in recent decades in this region (Kim et al. 2014).

The processes of denitrification, N_2 fixation, and atmospheric N deposition are all believed to be crucial to regulating the distribution of DIP and its excess relative to dissolved inorganic nitrogen (DIN) in surface waters of the low latitude oceans (Gruber and Sarmiento 1997; Wu et al. 2000; Kim et al. 2014). For example, in the (sub)tropical North Atlantic, enhanced N_2 fixation in particular has been proposed as an essential driver of DIP drawdown, which in turn has been related to elevated iron (Fe) supply rates from aerosol deposition (Wu et al. 2000; Moore et al. 2009). In contrast to the North Atlantic, high DIP concentrations in the South Atlantic have been suggested to reflect Fe limitation of N_2 fixation (Moore et al. 2009). A similar control has been suggested to drive a regional DIP gradient in the North Pacific (Hashihama et al. 2009; Kitajima et al. 2009; Shiozaki et al. 2010).

Microbial communities growing under scarce phosphorus (P) initiate a range of stress responses, including the substitution of phospholipids for non-phosphorus containing forms (Van Mooy et al. 2009), utilization of reduced P(III) species (phosphite and phosphonates; Van Mooy et al. 2015; Repeta et al. 2016), and upregulation of P scavenging enzymes including alkaline phosphatases (APases) for hydrolysis of dissolved organic phosphorus (DOP) (Karl 2014). In such regions, the concentrations of DOP can exceed DIP by orders of magnitude, with the labile components of this pool potentially supporting microbial P requirements and thereby overall productivity in these systems (Mather et al. 2008; Letscher et al. 2016). Subsequently, the ranges of microbially produced DOP acquisition enzymes have diverse trace metal requirements (Duhamel et al. 2021), presenting the possibility that the restricted availability of these elements could limit DOP acquisition rates in the ocean. For example, evidence has been found for Fe (Browning et al. 2017) and Zn (Mahaffey et al. 2014) limitation of APases activity (APA) in the tropical North Atlantic. However, robust links between DIP availability, N_2 fixation, aerosol deposition, and the controls on microbial access to the DOP pool are lacking in the subtropical northwest Pacific, a vast ecosystem that is subject to rapid changes (e.g., Kavanaugh et al. 2018).

Here, we report results from simultaneous measurements of low-level macronutrient concentrations, trace elements, N_2 fixation and APA across the subtropical northwest Pacific, and supplement these with bioassay experiments testing the short-term microbial response to (micro-)nutrient supply. In parallel, desert dust and anthropogenically impacted aerosols, potentially releasing a range of (micro-)nutrients simultaneously, were further supplied in experiments to simulate the potential short-term biogeochemical impact of their supply.

Methods

Experiments and sample collection were conducted onboard RV *Tan Kah Kee* from 7th to 18th January 2021 (Fig. 1a). Surface seawater for amendment experiments and ambient nutrient and trace metal concentrations measurements (3-h time interval) was pumped from ~ 2 m depth into a trace-metal-clean laboratory from a towed sampling device (Zhang et al. 2019). Additional discrete depth profile samples were collected throughout the upper 1000 m using 12-L Niskin sampling bottles alongside a conductivity–temperature–depth (CTD) profiler. The photosynthetically active radiation (PAR) sensor attached to the CTD was used to evaluate 1% of the surface PAR depth (euphotic zone, Lee et al. 2007) and 0.1% of the surface PAR depth.

Nutrient and aerosol amendment experiments were carried out at four sites near the corresponding stations. Bottled seawater samples (1 L acid-washed polycarbonate bottles; Nalgene) were spiked in triplicate with N (1 μmol L^{-1} $NO_3^- + 1$ μmol L^{-1} NH_4^+), P (0.1 μmol L^{-1} PO_4^{3-}), Fe (5 nmol L^{-1} Fe^{3+}), Cu (1 nmol L^{-1} Cu^{2+}), Zn (5 nmol L^{-1} Zn^{2+}), Ni (1 nmol L^{-1} Ni^{2+}) and a number of combinations (P + Fe, P + Ni, N + P, N + Cu, N + Fe, N + Fe + Cu), and with different types of aerosols (aerosols comprised of desert-type dust [A1] and anthropogenic perturbed aerosol [A2], each at 0.02 and 0.2 mg L^{-1}, referred to as A1_0.02, A1_0.2, A2_0.02, and A2_0.2, respectively). Triplicate control bottles without nutrient amendment were also collected. All bottles were capped and placed in on-deck incubators connected to the ship's underway flow-through system to continuously flushed

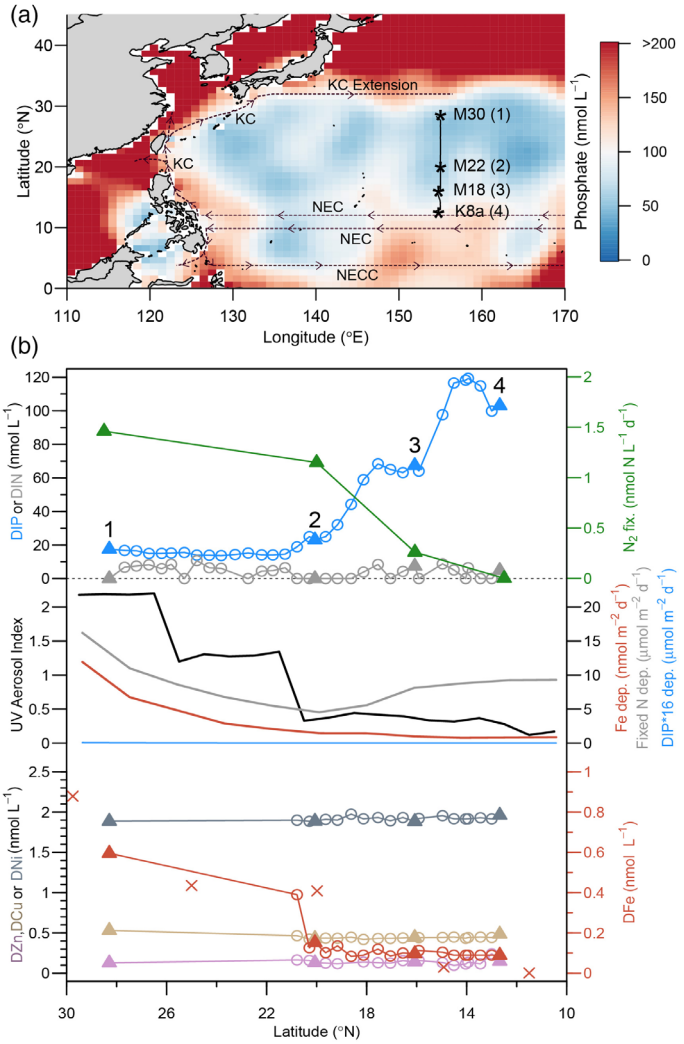

Fig. 1. Study sites and nutrient distributions. (**a**) Map of the western North Pacific Ocean showing the sampling and experimental sites (asterisks) along a meridional transect at 155°E. The background colors represent surface phosphate concentrations from the World Ocean Atlas. Mean surface currents are shown (Talley et al. 2011): NEC, North Equatorial Current; NECC, North Equatorial Counter Current; KC, Kuroshio Current. (**b**) Meridional nutrient and aerosol trends. DIP = dissolved inorganic phosphorus; DIN = dissolved inorganic nitrogen; N_2 fix = N_2 fixation rate; UV aerosol index is the satellite-derived average during the cruise (7^{th}–18^{th} January 2021); climatological model estimates of nutrient deposition are expressed as Fe deposition, fixed N deposition, and DIP deposition × 16 (scaling to typical phytoplankton N : P); DZn = dissolved zinc; DFe = dissolved iron; DCu = dissolved copper; and DNi = dissolved nickel. Sampling locations are highlighted with open circles and filled triangles indicating the start point locations of the bioassay experiments. Trace metal samples around 21–28°N were not collected. Surface DFe concentrations along the same transect from Nishioka et al. (2020) are shown as crosses.

with surface waters. After ~ 48 h incubation, experiments were taken down and subsampled for chlorophyll *a* measurements (all triplicate replicates) and APA (replicate rate measurements made from one of the triplicate incubation bottles).

All laboratory analysis details are provided in Supporting Information Text S1. The monthly average climatology for surface phosphate concentration was obtained from the World Ocean Altas 2018 (https://www.ncei.noaa.gov/products/world-ocean-atlas). The satellite-derived average UV aerosol index was downloaded from GIOVANNI (https://giovanni.gsfc.nasa.gov/giovanni). Daily sea level anomaly was obtained from the Copernicus Climate Data Store (https://cds.climate.copernicus.eu/cdsapp#!/dataset/satellite-sea-level-global?tab=overview). Aerosol depositions of Fe, fixed N, and DIP were extracted from the published model result of Chien et al. (2016).

Results and discussion

The cruise track transited the North Pacific Subtropical Gyre, from the northern boundary to its southern extent at the north equatorial current (NEC) (Fig. 1a). Surface waters were consistently depleted in DIN (mean DIN = 3.8 nmol L^{-1}, SD = 3.6 nmol L^{-1}, n = 34). In contrast to DIN, DIP displayed a pronounced gradient, increasing more than fivefold from ~ 20 nmol L^{-1} in the north to > 100 nmol L^{-1} in the south of the study area (Fig. 1b; Table 1). This trend is consistent with the overall pattern in climatological values from the WOA dataset (Fig. 1a) alongside other previous observations (Hashihama et al. 2009, 2021; Kitajima et al. 2009; Shiozaki et al. 2010; Martiny et al. 2019). Surface N_2 fixation rates measured at the four stations demonstrated an opposite trend to that of surface DIP concentrations, with rates decreasing abruptly between the two northerly stations (1.46 and 1.15 nmol L^{-1} d^{-1} at Stas. M30 and M22, respectively) and two stations in the south (0.26 and 0 nmol L^{-1} d^{-1} at Stas. M18 and K8a, respectively). Although our number of N_2 fixation observations is restricted, the inverse gradients in N_2 fixation rates and DIP concentrations between the gyre circulation and the NEC in the western (sub)tropical Pacific have consistently been observed in prior studies (Hashihama et al. 2009; Kitajima et al. 2009; Shiozaki et al. 2010).

Our observed gradients in DIP and N_2 fixation were also consistent with that documented in the (sub)tropical Atlantic, where a major aerosol Fe deposition gradient regulates where N_2 fixers, with exceptionally high Fe requirements, can become established (Moore et al. 2009). A similar mechanism has been proposed for the gradients observed in the western (sub)tropical Pacific (Hashihama et al. 2009; Kitajima et al. 2009; Shiozaki et al. 2010). In this study, concentrations of dissolved Fe were measured along parts of the transect, which demonstrated an elevated value in the northern-most site (0.60 nmol L^{-1}; Sta. M30) that exceeded values further to the south approximately twofold to sixfold (Fig. 1b; Table 1). Overall, this agreed very well with previous results along exactly the same transect (Nishioka et al. 2020), although differed somewhat to less clear trends found further to the east (Tanita et al. 2021); the latter potentially reflective of the

Table 1. Initial conditions of the bioassay experiments.

Experiment	1	2	3	4
Longitude (°E)	155	155	155	155
Latitude (°N)	28.5	20	16	12.5
SST (°C)	22.3	27.8	27.9	27.9
Salinity	34.7	35.0	34.7	34.3
SLA (m)	0.09	0.11	0.17	0.14
DIN (nmol L^{-1})*	0†	0†	7.4	4.9†
$F_{\_DIN}$ (μmol m^{-2} d^{-1})‡	32.9	6.6	5.3	8.5
DIP (nmol L^{-1})	17.5	23.1	67.4	103.1
$F_{\_DIP}$ (μmol m^{-2} d^{-1})‡	1.49	0.36	0.30	0.55
$F_{\_DIN}$: $F_{\_DIP}$	22	18	18	15
NH_4^+ (nmol L^{-1})§	3.3	9.1	3.6	1.2†
DSi (μmol L^{-1})	1.52	0.95	1.08	1.20
Fe (nmol L^{-1})	0.60	0.15	0.10	0.09
Zn (nmol L^{-1})	0.13	0.13	0.14	0.15
Cu (nmol L^{-1})	0.53	0.43	0.45	0.49
Ni (nmol L^{-1})	1.89	1.89	1.88	1.96
N_2 fix (nmol N L^{-1} d^{-1})	1.46±0.24	1.15±0.12	0.26±0.03	0±0†
Chl *a* (μg L^{-1})	0.22	0.07	0.10	0.07

*Here, DIN represents nitrate + nitrite.
†Below detection limit (DIN = 5.2 nmol L^{-1}, NH_4^+ = 2.3 nmol L^{-1}, N_2 fix = 0.22 nmol N L^{-1} d^{-1}).
‡Upward fluxes at 0.1% surface PAR.
§Determined at nearby sampling stations.

episodic nature of aerosol deposition and the relatively short lifetime of Fe in surface waters. This trend was generally consistent with enhanced Fe availability for N_2 fixation in the northern sites. To further investigate if this trend was related to enhanced aerosol deposition, we analyzed satellite observations of UV aerosol index, a proxy for atmospheric aerosol loading, for the time of our cruise (Torres et al. 2013) and published climatological model estimates of nutrient deposition (Chien et al. 2016). Both the UV aerosol index and model Fe deposition displayed a trend consistent with enhanced aerosol Fe deposition in the north, with more than fourfold greater atmospheric aerosol loading indicated by the UV index and greater than fourfold higher aerosol Fe deposition in the northern (M30 and M22) compared to southern (M18 and K8a) stations. Concentrations of dissolved Zn, Cu, and Ni concentrations showed much less variability than Fe, with the average values of 0.14, 0.45, and 1.92 nmol L^{-1}, respectively (Fig. 1b; Table 1), consistent with aerosols probably being a less important source of these elements (Mahowald et al. 2018).

In line with the highly depleted DIN concentration throughout the transect (Fig. 1b), nutrient addition experiments conducted at the four stations demonstrated that N was always the primary limiting nutrient for the bulk phytoplankton community (Fig. 2). No Chl *a* enhancements were observed following the addition of any nutrient combination that did not contain N, including those amended with P, Fe, Cu, Zn, or Ni. At the northernmost station (M30, Experiment 1), which was host to the highest N_2 fixation rates and the lowest DIP concentrations (Table 1), serial Chl *a* enhancement (that is, a greater response to the addition of N alone) was observed following addition of N + P and N + Fe combinations. The serial response to P addition can be readily explained, reflecting a condition where depleted initial seawater DIP concentrations (17.5 nmol L^{-1}) are further lowered to limiting levels following artificial addition of bioavailable N (Moore et al. 2008; Browning et al. 2017, 2022). In contrast, the serial limitation response to N + Fe is less easy to reconcile with the elevated dissolved Fe concentrations at this site (0.60 nmol L^{-1}). Furthermore in Experiment 1, no significant Chl *a* enhancement was observed following the addition of N + Fe + Cu, suggesting that the Cu addition prevented stimulation of phytoplankton growth (Paytan et al. 2009); however, this was difficult to reconcile with the significant enhancements that were observed in Experiments 2–4. The addition of the variety of aerosol treatments appeared to relieve the primary N limitation at all sites, by enhancing Chl *a* to levels observed in N addition treatments, suggesting both types of aerosols at both loading concentrations supplied bioavailable N (Fig. S1).

In addition to the depleted concentrations of DIP in the upper water column (Fig. 3c), alongside the serial Chl

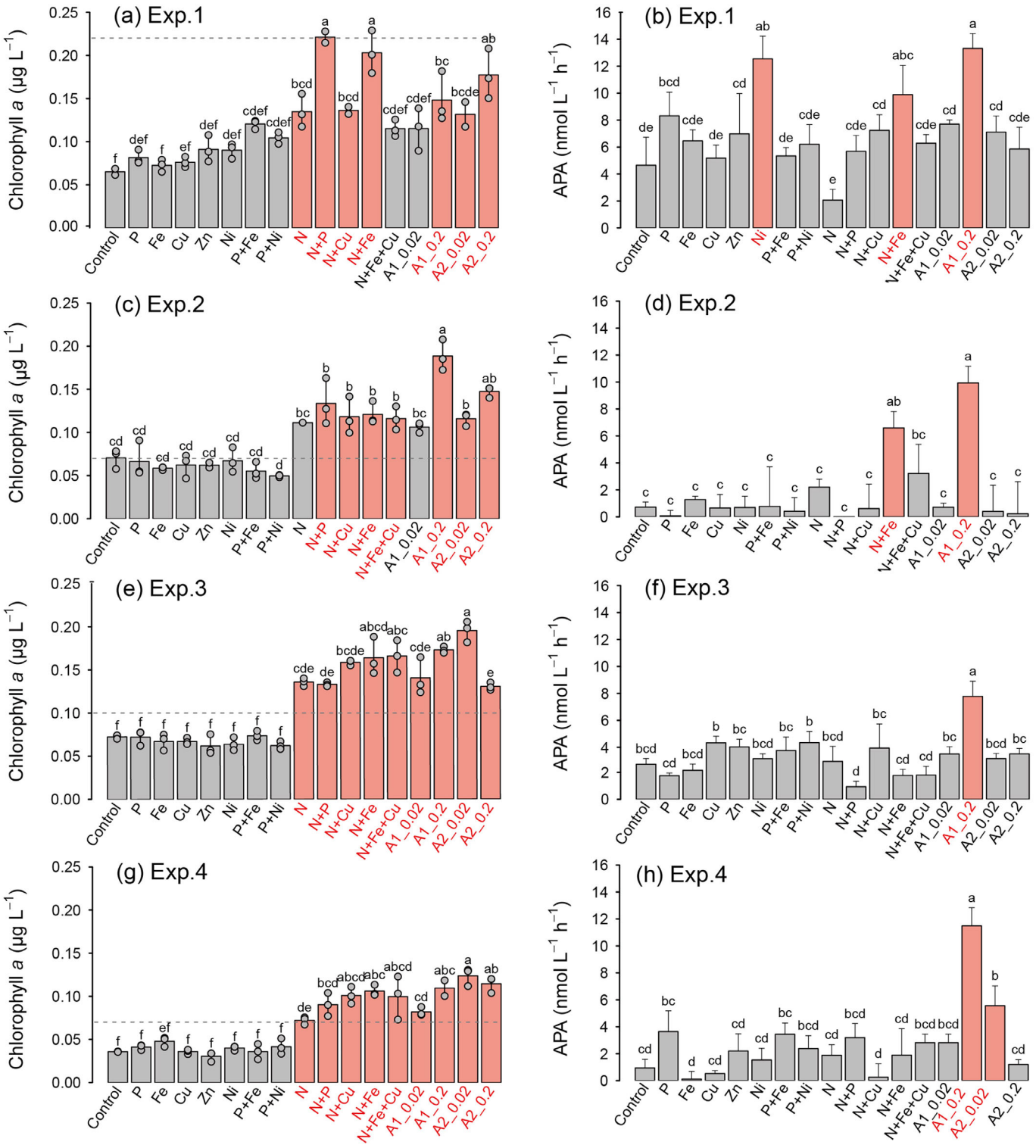

Fig. 2. Microbial responses to nutrient and aerosol amendments. Chlorophyll *a* (**a**, **c**, **e**, **g**). Points denote individual values; bar heights and lines indicate the means and ranges, respectively ($n = 3$). Horizontal dashed lines represent initial values. Alkaline phosphate activity (**b**, **d**, **f**, **h**). Bar heights and lines indicate the means and standard errors, respectively ($n = 3$). The added aerosols comprised of desert-type dust [A1] and anthropogenic perturbed aerosol [A2], each at 0.02 and 0.2 mg L^{-1}, referred to as A1_0.02, A1_0.2, A2_0.02, and A2_0.2, respectively. The sample of zinc (Zn) addition in Experiment 2 was not determined. Statistically distinguishable means are labeled with different letters (using a one-way ANOVA and a Tukey honest significant difference [HSD] means comparison test, $p < 0.05$). The red bars and labels indicate that the treatments are significantly increased relative to controls.

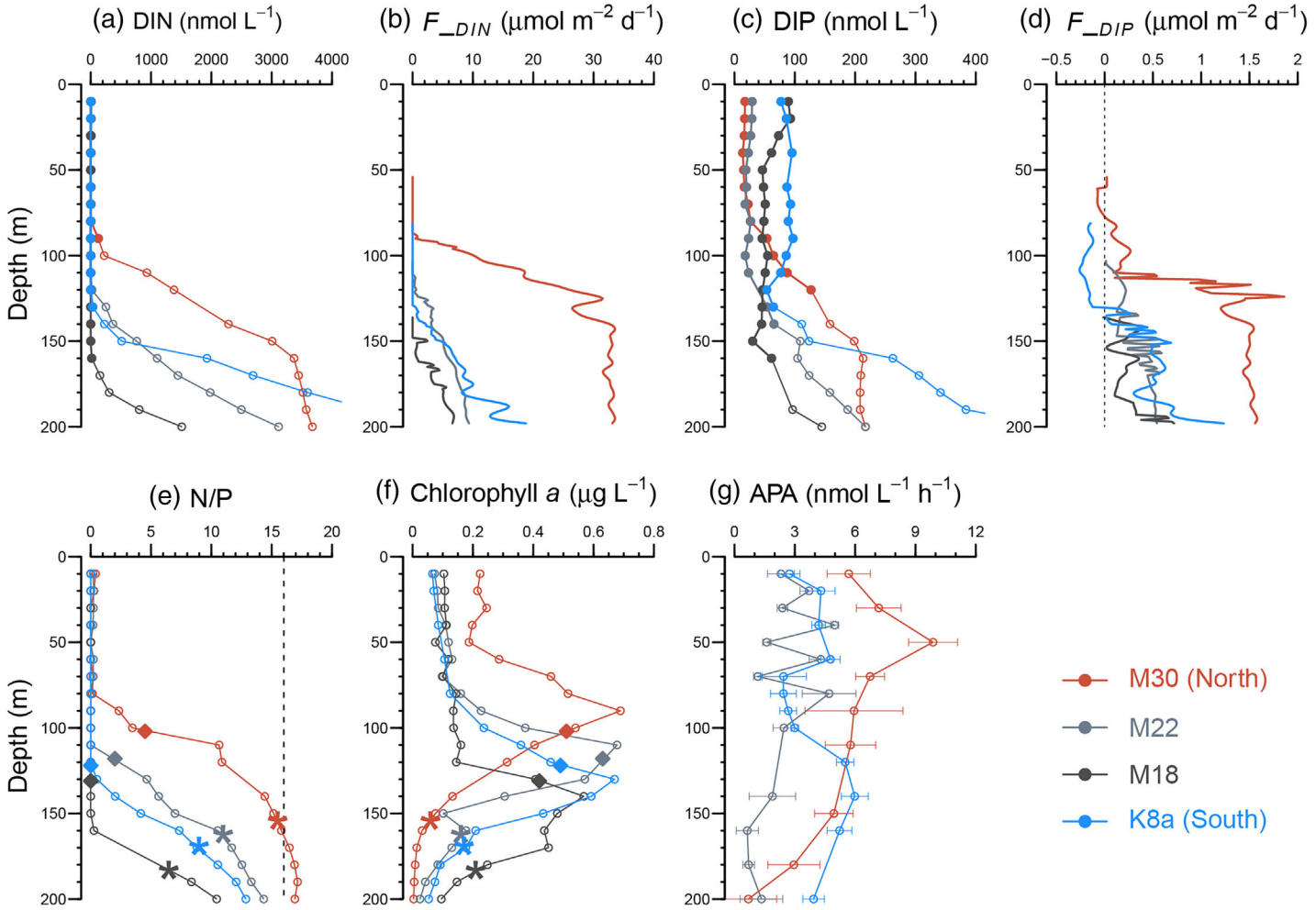

Fig. 3. Depth profiles of biogeochemical parameters at four sampling stations. (**a**) DIN concentration; (**b**) diapycnal fluxes of DIN, F_DIN; (**c**) DIP concentration; (**d**) diapycnal fluxes of DIP, F_DIP; (**e**) N/P ratio. Vertical dashed line represents the Redfield N/P ratio of 16 : 1 (Redfield et al. 1963); (**f**) chlorophyll *a* concentration; and (**g**) rate of APA. Error bars represent the standard errors of triplicates. Nutrients measured via the AA3 Auto-Analyzer and nanomolar techniques are distinguished by open circles and filled circles, respectively. Diamonds and asterisks in (**e**) and (**f**) indicate 1% surface PAR and 0.1% surface PAR, respectively.

a enhancement to N + P supply at the northern station (M30; Fig. 2a), evidence for in situ P stress was provided by rates of APA (Fig. 3g). Rates of APA were enhanced approximately two-fold in surface waters at northern sites, and more broadly throughout the upper water column (matching previous observations in the region; Suzumura et al. 2012), likely suggesting more rapid utilization of DOP in these waters. Across the whole dataset, APA rates were generally inversely correlated with DIP concentrations (Fig. S3). This matches previous observations (Lomas et al. 2010; Suzumura et al. 2012; Mahaffey et al. 2014), although we observed substantial variations in this trend, including cases where APA was elevated but DIP concentrations were not depleted (Fig. S3; Sebastián et al. 2004; Duhamel et al. 2011; Davis and Mahaffey 2017). Responses of APA to nutrient addition were thus less clear than that for Chl *a*, however some broad trends emerged. First, in contrast to several previous observations (Tanaka et al. 2006; Duhamel et al. 2010; Mahaffey et al. 2014; Browning et al. 2017), but consistent with depth profiles (Fig. 3c,g), P addition did not suppress rates of APA. Nitrogen and Fe addition at the northern, most P-depleted sites led to significant APA increases relative to untreated controls (Fig. 2b,d), presumably due to (1) stimulating phytoplankton growth by the provision of the primary limiting nutrient (N) and thereby further decreasing DIP concentrations, but also (2) provision of Fe, which is a required cofactor for widespread forms of APases enzymes (PhoX and PhoD; Luo et al. 2009; Rodriguez et al. 2014; Yong et al. 2014). Moreover, additions of high concentration of desert-type aerosol (A1_0.2) consistently elevated APA across all experiments (Fig. 2b,d,f,h). This could not be reconciled with the higher amounts of Fe and fixed N being supplied

from A1_0.2 (Fig. S1), as the parallel N + Fe treatment was already to replete values for both nutrients, but did not initiate APA responses at the southerly sites (Fig. 2f,h). Alternatively, the supply of aerosols might have also supplied significant labile organic carbon, which could have increased concentrations and activity of heterotrophic bacteria and thereby APA (Nicholson et al. 2006; Cao et al. 2010; Luo et al. 2011). Finally, the reason for the significant increase in APA after Ni addition at Experiment 1 was not clear, as Ni neither led to an increase in Chl *a* concentrations nor has a known role in APases (Duhamel et al. 2021). Ni is a cofactor in urease, which could have increased urea utilization as an N source, leading to P drawdown and thereby the increases in APA; however, such a mechanism would be expected to be associated with an increase in Chl *a* concentrations following Ni addition, which were not observed.

Ultimately, the relative supply rate of bioavailable N vs. P to the euphotic upper ocean would set how close P becomes to be limiting phytoplankton growth, with denitrification, N_2 fixation, and atmospheric deposition playing major roles (Gruber and Sarmiento 1997; Wu et al. 2000; Kim et al. 2014). Model aerosol nutrient deposition values for our transect suggest that aerosols supply both more Fe and fixed N to the northern part of the region, while the aerosol supply of DIP is predicted to be negligible, consistent with observations (Fig. 1b; Table S1; Baker et al. 2010; Martino et al. 2014). Iron stimulation of N_2 fixation, in combination with the direct aerosol supply of fixed N, will both partially relieve N limitation of the bulk phytoplankton community in the north, contributing to the drawdown in surface DIP concentrations in conjunction with the increase in Chl *a* concentrations (Fig. 3; Table 1). However, estimating the depth-integrated N_2 fixation rate by either integrating the measured surface N_2 fixation rates through the entire euphotic zone, or using published relationships between surface ($\rho_{surface}$) and depth-integrated ($\int\rho$) N_2 fixation rates ($\int\rho = 61.4\,\rho_{surface}$, $r^2 = 0.92$, $n = 22$, $p < 0.001$; Wen et al. 2022), produces a new N supply from N_2 fixation of either 142 or 80 μmol N m^{-2} d^{-1}, respectively (Table S1). Either of these values is an order of magnitude higher than the estimated model aerosol N deposition ($\sim$9 μmol N m^{-2} d^{-1}). Therefore, acknowledging the caveat of poor data constraint on both N supply terms, this points toward N_2 fixation being the dominant N supply mechanism leading to P drawdown. A fingerprint of this elevated N input is furthermore potentially reflected in the concentrations of DIN and DIP below the euphotic zone (Figs. 3, S4). Ratios of N : P concentrations are elevated in the northern sites relative to the south at the base of the euphotic layer, or 0.1% surface PAR depth, potentially reflecting the accumulation of diazotroph-derived DIN below the euphotic zone (Gruber and Sarmiento 1997; Wu et al. 2000; Kim et al. 2014), although the role of advection of subsurface waters with elevated N : P ratios from elsewhere cannot be ruled out. Upward effective diapycnal fluxes from these relatively N-enriched subsurface waters into the euphotic zone will act to further sustain the latitudinal surface DIP gradient (ratios of N : P fluxes at the 0.1% surface PAR depth, $F_{\_DIN} : F_{\_DIP}$, decreasing from 22 in the north to 15 in the south; Table 1). As a result, the reduced supply of DIP into the euphotic zone, relative to N, would thus drive the northern microbial community being more reliant on the rapid internal recycling of P (Fig.3g; Hashihama et al. 2021; including unmeasured forms of reduced P).

We reconcile the broadscale meridional phosphate gradient through the western subtropical North Pacific (Hashihama et al. 2009; Kitajima et al. 2009; Shiozaki et al. 2010; Martiny et al. 2019) with (1) primary N limitation of the bulk phytoplankton community, and (2) aerosol Fe regulating the latitudinal distribution of N_2 fixation rates, which introduces new bioavailable nitrogen and leads to phosphate drawdown (Wu et al. 2000; Hashihama et al. 2009). Secondary mechanisms likely contribute to the consistency of the low phosphate throughout the northern region despite more expected variability in aerosol Fe deposition and N_2 fixation (Fig. 1b); including direct aerosol supply of N, sustained upward diffusion of elevated N : P (ultimately derived from enhanced N_2 fixation in waters above) and potentially also Fe (ultimately aerosol-derived, but accumulated in the subsurface; Conway and John 2014; Rigby et al. 2020), alongside lateral advection and mixing of waters throughout the region (Lomas et al. 2010; Martiny et al. 2019). Phosphate depletion in the northern part of the study region in the season of the present study led to enhanced rates of APA and serial limitation of the bulk phytoplankton community by P, suggesting that the system is potentially approaching a state of N-P colimitation. Building on the observations presented here, future work employing lower-level nutrient addition experiments combined with simultaneous assessments of N_2 fixation rates and nutrient concentrations would further resolve just how close this system is to N–P colimitation. Regardless, enhanced N supply without equivalent P, via aerosol N deposition or N_2 fixation, would further draw down surface phosphate, strengthen P stress, and enhance microbial reliance on the DOP pool for phosphate (Lomas et al. 2010). However, while the contributions of N_2 fixation and atmospheric N supply to phytoplankton growth, and subsequent phosphate drawdown, are additive on short timescales, they have the potential to become strongly decoupled if enhanced aerosol N inputs reduce the niche for diazotrophs, via competition with non-diazotrophs for P and/or Fe (Krishnamurthy et al. 2007). Increasing aerosol N inputs to the North Pacific have been documented (Kim et al. 2014), underscoring the need to better understand the biogeochemical impacts of this forcing. Observations such as those presented here are a starting point for making such assessments.

References

Baker, A. R., T. Lesworth, C. Adams, T. D. Jickells, and L. Ganzeveld. 2010. Estimation of atmospheric nutrient inputs to the Atlantic Ocean from 50°N to 50°S based on large-scale field sampling: Fixed nitrogen and dry deposition of phosphorus. Glob. Biogeochem. Cycles **24**: GB3006. doi:10.1029/2009GB003634

Browning, T. J., E. P. Achterberg, J. C. Yong, I. Rapp, C. Utermann, A. Engel, and C. M. Moore. 2017. Iron limitation of microbial phosphorus acquisition in the tropical North Atlantic. Nat. Commun. **8**: 15465. doi:10.1038/ncomms15465

Browning, T. J., and others. 2022. Nutrient co-limitation in the subtropical Northwest Pacific. Limnol. Oceanogr.: Lett. **7**: 52–61. doi:10.1002/lol2.10205

Cao, X., C. Song, and Y. Zhou. 2010. Limitations of using extracellular alkaline phosphatase activities as a general indicator for describing P deficiency of phytoplankton in Chinese shallow lakes. J. Appl. Phycol. **22**: 33–41. doi:10.1007/S10811-009-9422-0

Chien, C. T., K. R. M. Mackey, S. Dutkiewicz, N. M. Mahowald, J. M. Prospero, and A. Paytan. 2016. Effects of African dust deposition on phytoplankton in the western tropical Atlantic Ocean off Barbados. Glob. Biogeochem. Cycles **30**: 716–734. doi:10.1002/2015GB005334

Conway, T. M., and S. G. John. 2014. Quantification of dissolved iron sources to the North Atlantic Ocean. Nature **511**: 212–215. doi:10.1038/nature13482

Davis, C. E., and C. Mahaffey. 2017. Elevated alkaline phosphatase activity in a phosphate-replete environment: Influence of sinking particles. Limnol. Oceanogr. **62**: 2389–2403. doi:10.1002/LNO.10572

Duhamel, S., S. T. Dyhrman, and D. M. Karl. 2010. Alkaline phosphatase activity and regulation in the North Pacific Subtropical Gyre. Limnol. Oceanogr. **55**: 1414–1425. doi:10.4319/lo.2010.55.3.1414

Duhamel, S., K. M. Björkman, F. van Wambeke, T. Moutin, and D. M. Karl. 2011. Characterization of alkaline phosphatase activity in the north and south pacific subtropical gyres: Implications for phosphorus cycling. Limnol. Oceanogr. **56**: 1244–1254. doi:10.4319/LO.2011.56.4.1244

Duhamel, S., J. M. Diaz, J. C. Adams, K. Djaoudi, V. Steck, and E. M. Waggoner. 2021. Phosphorus as an integral component of global marine biogeochemistry. Nat. Geosci. **14**: 359–368. doi:10.1038/s41561-021-00755-8

Gruber, N., and J. L. Sarmiento. 1997. Global patterns of marine nitrogen fixation and denitrification. Glob. Biogeochem. Cycles **11**: 235–266. doi:10.1029/97GB00077

Hashihama, F., K. Furuya, S. Kitajima, S. Takeda, T. Takemura, and J. Kanda. 2009. Macro-scale exhaustion of surface phosphate by dinitrogen fixation in the western North Pacific. Geophys. Res. Lett. **36**: L03610. doi:10.1029/2008GL036866

Hashihama, F., and others. 2021. Nanomolar phosphate supply and its recycling drive net community production in the subtropical North Pacific. Nat. Commun. **12**: 3462. doi:10.1038/s41467-021-23837-y

Karl, D. M. 2014. Microbially mediated transformations of phosphorus in the sea: New views of an old cycle. Ann. Rev. Mar. Sci. **6**: 279–337. doi:10.1146/ANNUREV-MARINE-010213-135046

Kavanaugh, M. T., M. J. Church, C. O. Davis, D. M. Karl, R. M. Letelier, and S. C. Doney. 2018. ALOHA from the edge: Reconciling three decades of in situ eulerian observations and geographic variability in the North Pacific Subtropical Gyre. Front. Mar. Sci. **5**: 130. doi:10.3389/fmars.2018.00130

Kim, I. N., K. Lee, N. Gruber, D. M. Karl, J. L. Bullister, S. Yang, and T. W. Kim. 2014. Increasing anthropogenic nitrogen in the North Pacific Ocean. Science **346**: 1102–1106. doi:10.1126/science.1258396

Kitajima, S., K. Furuya, F. Hashihama, S. Takeda, and J. Kanda. 2009. Latitudinal distribution of diazotrophs and their nitrogen fixation in the tropical and subtropical western North Pacific. Limnol. Oceanogr. **54**: 537–547. doi:10.4319/LO.2009.54.2.0537

Krishnamurthy, A., J. K. Moore, C. S. Zender, and C. Luo. 2007. Effects of atmospheric inorganic nitrogen deposition on ocean biogeochemistry. J. Geophys. Res. Biogeo. **112**: 2019. doi:10.1029/2006JG000334

Lee, Z. P., A. Weidemann, J. Kindle, R. Arnone, K. L. Carder, and C. Davis. 2007. Euphotic zone depth: Its derivation and implication to ocean-color remote sensing. J. Geophys. Res.: Oceans **112**: C03009. doi:10.1029/2006JC003802

Letscher, R. T., F. Primeau, and J. K. Moore. 2016. Nutrient budgets in the subtropical ocean gyres dominated by lateral transport. Nat. Geosci. **9**: 815–819. doi:10.1038/ngeo2812

Lomas, M. W., A. L. Burke, D. A. Lomas, D. W. Bell, C. Shen, S. T. Dyhrman, and J. W. Ammerman. 2010. Sargasso Sea phosphorus biogeochemistry: An important role for dissolved organic phosphorus (DOP). Biogeosciences **7**: 695–710. doi:10.5194/bg-7-695-2010

Luo, H., R. Benner, R. A. Long, and J. Hu. 2009. Subcellular localization of marine bacterial alkaline phosphatases. Proc. Natl. Acad. Sci. USA **106**: 21219–21223. doi:10.1073/PNAS.0907586106

Luo, H., H. Zhang, R. A. Long, and R. Benner. 2011. Depth distributions of alkaline phosphatase and phosphonate utilization genes in the North Pacific Subtropical Gyre. Aquat. Microb. Ecol. **62**: 61–69. doi:10.3354/AME01458

Mahaffey, C., S. Reynolds, C. E. Davis, and M. C. Lohan. 2014. Alkaline phosphatase activity in the subtropical ocean: Insights from nutrient, dust and trace metal addition experiments. Front. Mar. Sci. **1**: 73. doi:10.3389/fmars.2014.00073

Mahowald, N. M., D. S. Hamilton, K. R. M. Mackey, J. K. Moore, A. R. Baker, R. A. Scanza, and Y. Zhang. 2018. Aerosol trace metal leaching and impacts on marine

microorganisms. Nat. Commun. **9**: 2614. doi:10.1038/s41467-018-04970-7

Martino, M., D. Hamilton, A. R. Baker, T. D. Jickells, T. Bromley, Y. Nojiri, B. Quack, and P. W. Boyd. 2014. Western Pacific atmospheric nutrient deposition fluxes, their impact on surface ocean productivity. Glob. Biogeochem. Cycles **28**: 712–728. doi:10.1002/2013GB004794

Martiny, A. C., and others. 2019. Biogeochemical controls of surface ocean phosphate. Sci. Adv. **5**: 341–369. doi:10.1126/sciadv.aax0341

Mather, R. L., and others. 2008. Phosphorus cycling in the north and South Atlantic Ocean subtropical gyres. Nat. Geosci. **1**: 439–443. doi:10.1038/ngeo232

Moore, C. M., M. M. Mills, R. Langlois, A. Milne, E. P. Achterberg, J. La Roche, and R. J. Geider. 2008. Relative influence of nitrogen and phosphorus availability on phytoplankton physiology and productivity in the oligotrophic sub-tropical North Atlantic Ocean. Limnol. Oceanogr. **53**: 291–305. doi:10.4319/LO.2008.53.1.0291

Moore, C. M., and others. 2009. Large-scale distribution of Atlantic nitrogen fixation controlled by iron availability. Nat. Geosci. **2**: 867–871. doi:10.1038/ngeo667

Moore, C. M., and others. 2013. Processes and patterns of oceanic nutrient limitation. Nat. Geosci. **6**: 701–710. doi:10.1038/ngeo1765

Nicholson, D., S. Dyhrman, F. Chavez, and A. Paytan. 2006. Alkaline phosphatase activity in the phytoplankton communities of Monterey Bay and San Francisco Bay. Limnol. Oceanogr. **51**: 874–883. doi:10.4319/LO.2006.51.2.0874

Nishioka, J., H. Obata, H. Ogawa, K. Ono, Y. Yamashita, K. Lee, S. Takeda, and I. Yasuda. 2020. Subpolar marginal seas fuel the North Pacific through the intermediate water at the termination of the global ocean circulation. Proc. Natl. Acad. Sci. USA **117**: 12665–12673. doi:10.1073/pnas.2000658117

Paytan, A., K. R. M. Mackey, Y. Chen, I. D. Lima, S. C. Doney, N. Mahowald, R. Labiosa, and A. F. Post. 2009. Toxicity of atmospheric aerosols on marine phytoplankton. Proc. Natl. Acad. Sci. USA **106**: 4601–4605. doi:10.1073/PNAS.0811486106

Redfield, A. C., B. H. Ketchum, and F. A. Richards. 1963. The influence of organisms on the composition of seawater, p. 26–77. *In* M. N. Hill [ed.], The *Sea*, v. **2**. Interscience Publishers.

Repeta, D. J., S. Ferrón, O. A. Sosa, C. G. Johnson, L. D. Repeta, M. Acker, E. F. Delong, and D. M. Karl. 2016. Marine methane paradox explained by bacterial degradation of dissolved organic matter. Nat. Geosci. **9**: 884–887. doi:10.1038/ngeo2837

Rigby, S. J., R. G. Williams, E. P. Achterberg, and A. Tagliabue. 2020. Resource availability and entrainment are driven by offsets between nutriclines and winter mixed-layer depth. Glob. Biogeochem. Cycles **34**: e2019GB006497. doi:10.1029/2019GB006497

Rodriguez, F., J. Lillington, S. Johnson, C. R. Timmel, S. M. Lea, and B. C. Berks. 2014. Crystal structure of the *Bacillus subtilis* phosphodiesterase PhoD reveals an iron and calcium-containing active site. J. Biol. Chem. **289**: 30889–30899. doi:10.1074/jbc.M114.604892

Sebastián, M., J. Arístegui, M. F. Montero, J. Escanez, and F. X. Niell. 2004. Alkaline phosphatase activity and its relationship to inorganic phosphorus in the transition zone of the north-western African upwelling system. Prog. Oceanogr. **62**: 131–150. doi:10.1016/J.POCEAN.2004.07.007

Shiozaki, T., K. Furuya, T. Kodama, S. Kitajima, S. Takeda, T. Takemura, and J. Kanda. 2010. New estimation of N_2 fixation in the western and Central Pacific Ocean and its marginal seas. Glob. Biogeochem. Cycles **24**: GB1015. doi:10.1029/2009GB003620

Suzumura, M., F. Hashihama, N. Yamada, and S. Kinouchi. 2012. Dissolved phosphorus pools and alkaline phosphatase activity in the euphotic zone of the western North Pacific Ocean. Front. Microbiol. **3**: 99. doi:10.3389/fmicb.2012.00099

Talley, L. D., G. L. Pickard, W. J. Emery, and J. H. Swift. 2011. Pacific Ocean, p. 303–362. *In* L. D. Talley, G. L. Pickard, W. J. Emery, and J. H. Swift [eds.], *Descriptive physical oceanography: An introduction*. Academic Press. doi:10.1016/B978-0-7506-4552-2.10010-1

Tanaka, T., P. Henriksen, R. Lignell, K. Olli, J. Seppälä, T. Tamminen, and T. F. Thingstad. 2006. Specific affinity for phosphate uptake and specific alkaline phosphatase activity as diagnostic tools for detecting phosphorus-limited phytoplankton and bacteria. Estuaries Coasts **29**: 1226–1241. doi:10.1007/BF02781823

Tanita, I., T. Shiozaki, T. Kodama, F. Hashihama, M. Sato, K. Takahashi, and K. Furuya. 2021. Regionally variable responses of nitrogen fixation to iron and phosphorus enrichment in the Pacific Ocean. J. Geophys. Res. Biogeo. **126**: e2021JG006542. doi:10.1029/2021JG006542

Torres, O., C. Ahn, and Z. Chen. 2013. Improvements to the OMI near-UV aerosol algorithm using A-train CALIOP and AIRS observations. Atmos. Meas. Tech. **6**: 3257–3270. doi:10.5194/amt-6-3257-2013

Van Mooy, B. A. S., and others. 2009. Phytoplankton in the ocean use non-phosphorus lipids in response to phosphorus scarcity. Nature **458**: 69–72. doi:10.1038/nature07659

Van Mooy, B. A. S., and others. 2015. Major role of planktonic phosphate reduction in the marine phosphorus redox cycle. Science **348**: 783–785. doi:10.1126/science.aaa8181

Wen, Z., and others. 2022. Nutrient regulation of biological nitrogen fixation across the tropical western North Pacific. Sci. Adv. **8**: eabl7564. doi:10.1126/SCIADV.ABL7564

Wu, J., W. Sunda, E. A. Boyle, and D. M. Karl. 2000. Phosphate depletion in the Western North Atlantic Ocean. Science **289**: 759–762. doi:10.1126/science.289.5480.759

Yong, S. C., and others. 2014. A complex iron-calcium cofactor catalyzing phosphotransfer chemistry. Science **345**: 1170–1173. doi:10.1126/SCIENCE.1254237

Zhang, R., and others. 2019. Distribution of dissolved iron in the Pearl River (Zhujiang) estuary and the northern continental slope of the South China Sea. Deep-Sea Res. II: Top. Stud. Oceanogr. **167**: 14–24. doi:10.1016/J.DSR2.2018.12.006

Acknowledgments

This study is a contribution to Carbon-FE (Carbon Fixation and Export in oligotrophic ocean), a SOLAS endorsed project supported by the National Natural Science Foundation of China (Grants 41890804 and 41730533).

We thank the captain and other crew of R/V TKK for technical support during the GEOTRACES GPpr15 (KK2007) cruise. Tao Huang, Lifang Wang, Feipeng Xu, Ruotong Jiang, Hui Shen, Shujie Cai, and Yaoni Wang are thanked for their assistance in sample collection and/or analysis. Yanping Xu and Yaojin Chen are thanked for their logistical assistance. Z. Yuan was supported by the Chinese Scholarship Council through a joint PhD program (File No. 202106310003).

Submitted 14 May 2022
Revised 16 December 2022
Accepted 29 January 2023